

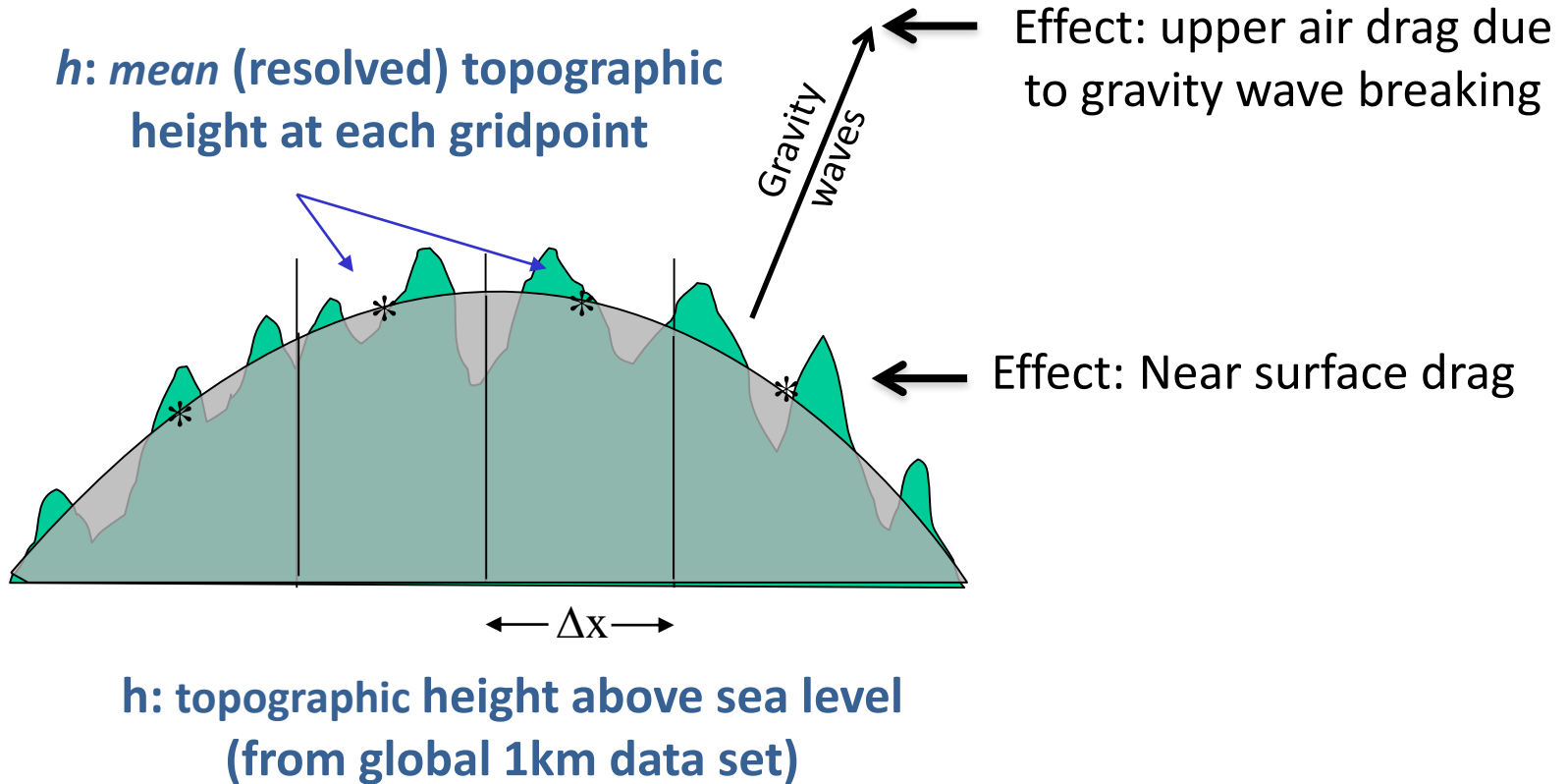
Parameterization of momentum fluxes related to sub-grid orography

Anton Beljaars

anton.beljaars@ecmwf.int
Room 016

- 1. Gravity wave theory**
- 2. Parameterization**
- 3. Impact**

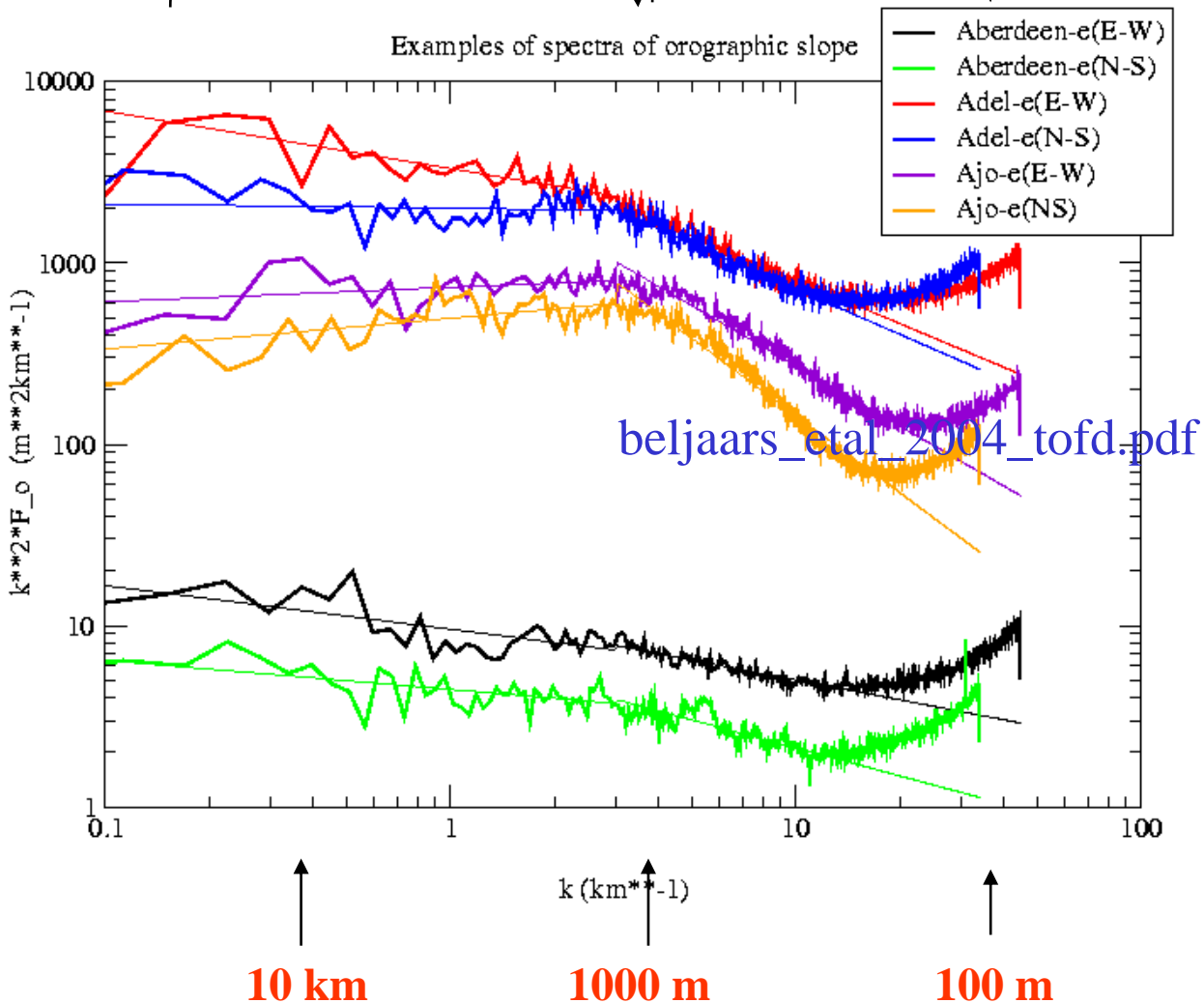
Sub-grid orography



Orographic slope spectrum

$$F(k) \sim k^{-1.9}$$

$$F(k) \sim k^{-2.8}$$



$$\theta^2 = \int_{k_o}^{\infty} k^2 F(k) dk$$

Simple properties of gravity waves

In order to prepare for a description of the parameterization of gravity-wave drag, we examine some simple properties of gravity waves excited by two-dimensional stably stratified flow over orography.

We suppose that the horizontal scales of these waves is sufficiently small that the Rossby number is large (ie Coriolis forces can be neglected), and the equations of motion can be written as

$$\frac{\partial u}{\partial t} + u \frac{\partial u}{\partial x} + w \frac{\partial u}{\partial z} + \frac{1}{\rho} \frac{\partial p}{\partial x} = 0 \quad (1)$$

$$\frac{\partial w}{\partial t} + u \frac{\partial w}{\partial x} + w \frac{\partial w}{\partial z} + \frac{1}{\rho} \frac{\partial p}{\partial z} + g = 0 \quad (2)$$

$$\frac{\partial u}{\partial x} + \frac{1}{\rho} \frac{\partial}{\partial z} (\rho w) = 0 \quad (3)$$

$$\frac{\partial \theta}{\partial t} + u \frac{\partial \theta}{\partial x} + w \frac{\partial \theta}{\partial z} = 0 \quad (4)$$

(After T. Palmer 'Theory of linear gravity waves', ECMWF meteorological training course, 2004)

Simple properties of gravity waves

The Boussinesq approximation is used whereby density is treated as a constant except where it is coupled to gravity in the buoyancy term of the vertical momentum equation. Linearising (1)-(4) about a uniform hydrostatic flow \mathbf{u}_0 with constant density ρ_0 and static stability \mathbf{N} , with

$$N^2 = g \frac{d \ln \theta_0(z)}{dz}, \quad \frac{dp_0}{dz} = -\rho_0 g,$$

$$u = u_0 + u', \quad w = 0 + w', \quad \rho = \rho_0 + \rho', \quad p = p_0 + p',$$

results in the perturbation variables

$$\frac{\partial u'}{\partial t} + u_0 \frac{\partial u'}{\partial x} + \frac{1}{\rho_0} \frac{\partial p'}{\partial x} = 0, \quad (5)$$

$$\frac{\partial w'}{\partial t} + u_0 \frac{\partial w'}{\partial x} + \frac{1}{\rho_0} \frac{\partial p'}{\partial z} - \frac{\rho'}{\rho_0} g = 0, \quad (6)$$

$$\frac{\partial u'}{\partial x} + \frac{\partial w'}{\partial z} = 0, \quad (7)$$

$$\frac{\partial \theta'}{\partial t} + u_0 \frac{\partial \theta'}{\partial x} + w' \frac{\partial \theta_0}{\partial z} = 0. \quad (8)$$

Simple properties of gravity waves

Assuming density fluctuations to be dependent on temperature only

$$\frac{\rho'}{\rho_0} = \frac{\theta'}{\theta_0}. \quad (9)$$

Equations (5-9) are five equations in five unknowns. These can be reduced to one linear equation

$$\left(\frac{\partial}{\partial t} + u_0 \frac{\partial}{\partial x} \right)^2 \left(\frac{\partial^2 w'}{\partial x^2} + \frac{\partial^2 w'}{\partial z^2} \right) + N^2 \frac{\partial^2 w'}{\partial x^2} = 0. \quad (10)$$

We now look for sinusoidal solutions of the general form

$$w' = \hat{w} \exp \left[i (kx + mz - \omega t) \right],$$

where

| | |
|----------------------|------------------------------|
| $k = 2\pi/\lambda_x$ | is the horizontal wavenumber |
| $m = 2\pi/\lambda_z$ | is the vertical wavenumber |
| ω | is the wave frequency |

Substitution leads to the dispersion relation

$$\left(\omega - u_0 k \right)^2 \left(k^2 + m^2 \right) - N^2 k^2 = 0,$$

$$\tilde{\omega} = \omega - u_0 k = \pm \frac{Nk}{\sqrt{k^2 + m^2}}.$$

$\tilde{\omega}$ is the intrinsic frequency

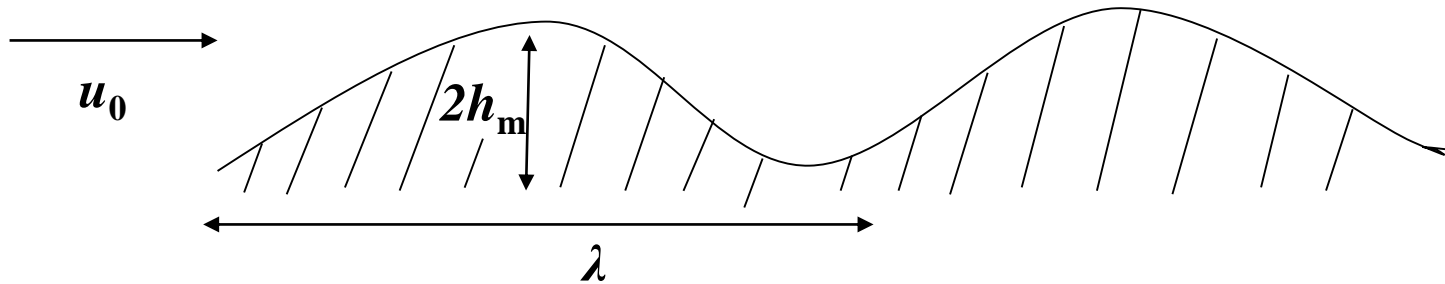
Derivation steps:

1. Use (9) to eliminate θ' from (8) -> resulting in equation for ρ' . Result: (8A)
2. Take total derivative of (6) and eliminate ρ' with (8A). Result: (6A)
3. Take total derivative of (5). Result (5A)
4. Take partial x-derivative of (6A) and subtract partial y-derivative of (5A). Result (6B).
5. Eliminate $\partial u/\partial x$ from (6B) using (7)

Sinusoidal hill

Consider stationary waves forced by sinusoidal orography with elevation $h(x)$

$$h = h_m \sin kx \quad k = 2\pi/\lambda$$



The lower boundary condition (the vertical component of the wind at the surface must vanish) is

$$w(z=0) = u_0 \frac{\partial h}{\partial x} = u_0 k h_m \cos kx$$

For steady state situations with $\omega=0$, m can be derived from the dispersion relation:

$$u_0^2 (k^2 + m^2) - N^2 = 0 \quad \rightarrow \quad m^2 = \frac{N^2}{u_0^2} - k^2$$

$$m^2 = N^2 / u_0^2 - k^2$$

Solutions periodic in x that satisfy the surface boundary condition:

$$w' = \text{Re} \left\{ \hat{w} e^{ikx + imz} \right\} = \text{Re} \left\{ u_0 k h_m e^{ikx + imz} \right\}$$

$$k > N/u_0$$

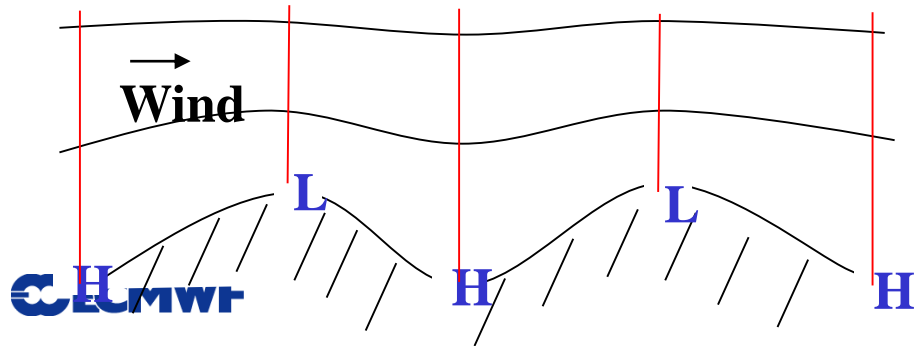
m is imaginary: Evanescent solution

$$w' = u_0 k h_m e^{-|m|z} \cos kx$$

From the continuity equation,

$$u' = u_0 h_m |m| e^{-|m|z} \sin kx$$

$$\overline{r_0 u' w'} = 0$$



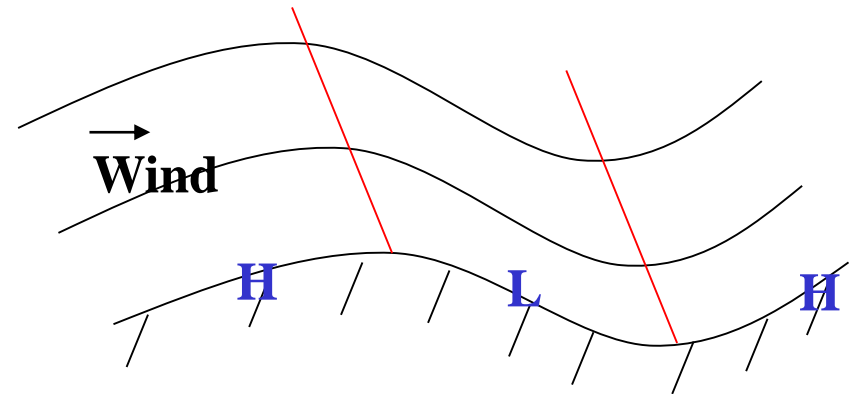
$$k < N/u_0$$

m is real: Propagating solution

$$w' = u_0 k h_m \cos(kx + mz)$$

$$u' = -u_0 m h_m \cos(kx + mz)$$

$$\overline{r_0 u' w'} = -0.5 r_0 u_0^2 k m h_m^2$$



Summary: two regimes

$k > N/U$ (i.e. narrow-ridge case)

(or equivalently $U\pi/L > N$, i.e. high frequency)

Evanescent solution (i.e. fading away)

Non-dimensional length $NL/U < \pi$

- waves decay exponentially with height
- vertical phase lines
- linear theory -> no drag. Steep small scales leading to form drag -> TOFD scheme

$$w = Ae^{-|m|z} \cos kx$$

$k < N/U$ (i.e. wider mountains)

(or equivalently $U\pi/L < N$, i.e. low frequency)

Wave solution

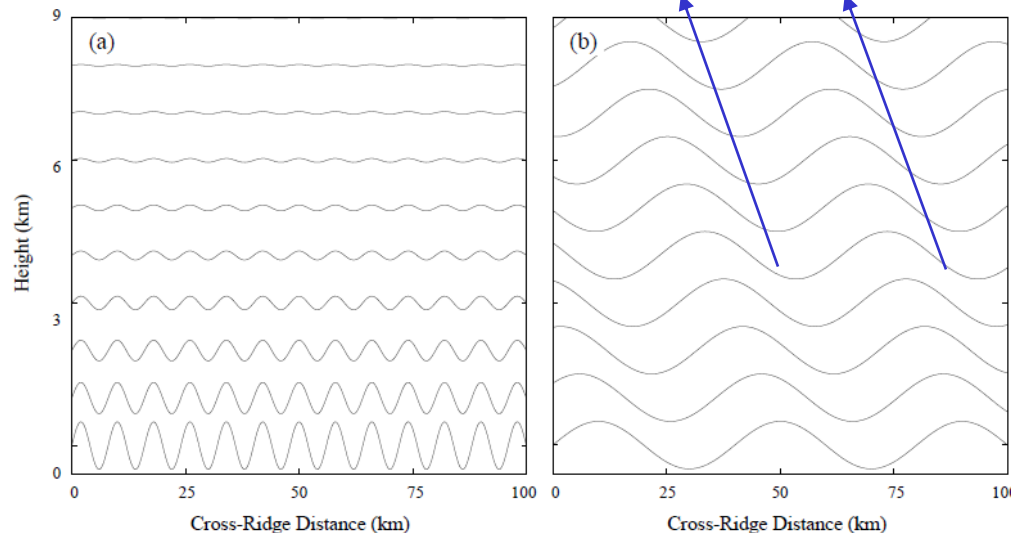
Non-dimensional length $NL/U > \pi$

- energy/momentum transported upwards
- waves propagate without loss of amplitude
- phase lines tilt upstream as z increases

$$w = A \cos(kx + mz)$$

For typical atmospheric wind and stability ($U=10$ m/s and $N=0.01$ s⁻¹):

$L \approx 3$ km



What happens to the moment flux associated with gravity waves

Momentum flux: $-\rho(\overline{u'w'})$
 is constant and density decreases with height,
 so the amplitude of gravity wave increases until
 they break

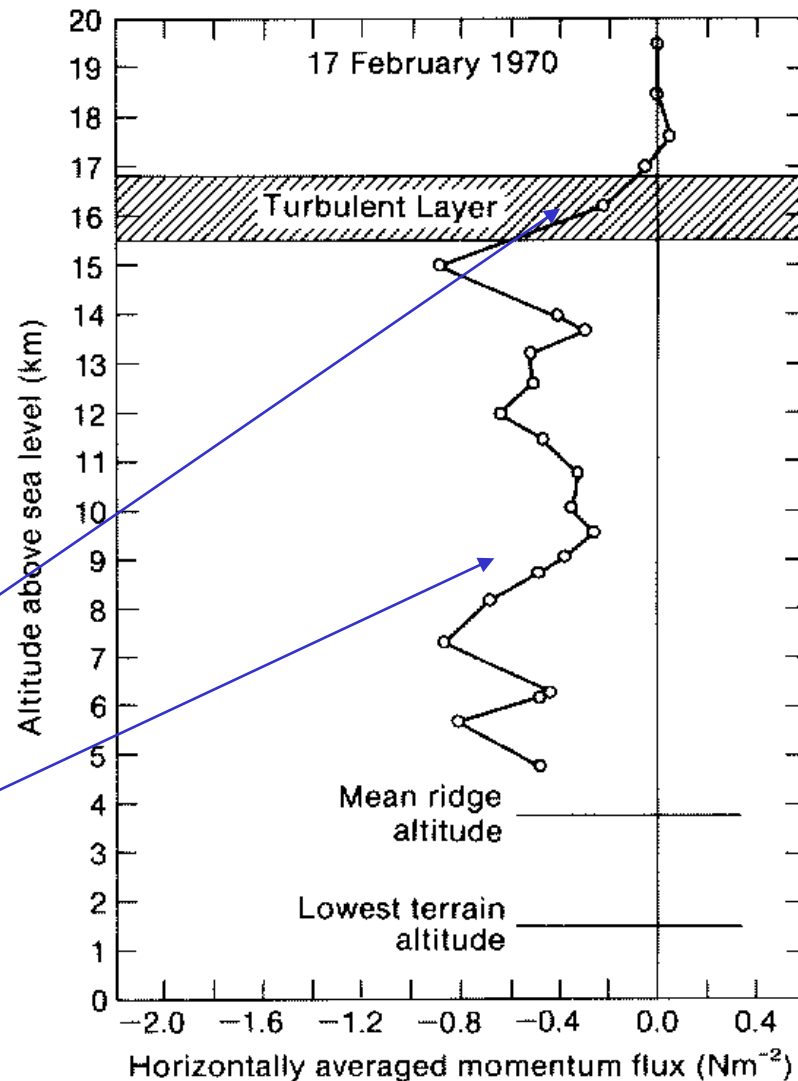
$$\frac{\partial u}{\partial t} = \frac{1}{\rho} \frac{\partial}{\partial z} (\rho \overline{u'w'})$$

**Stress rapidly changing; strong
 dissipation/wave breaking; $\partial u / \partial t \neq 0$**

**Stress largely unchanged; little
 dissipation/wave breaking; $\partial u / \partial t \approx 0$**

Wave breaking occurs:

1. When wave perturbation leads to convective overturning
2. Due to shear instability when locally the Richardson number drops below a critical value



Mean observed profile of momentum flux
 over Rocky mountains on 17 February 1970
 (from Lilly and Kennedy 1973)

Single lenticular cloud

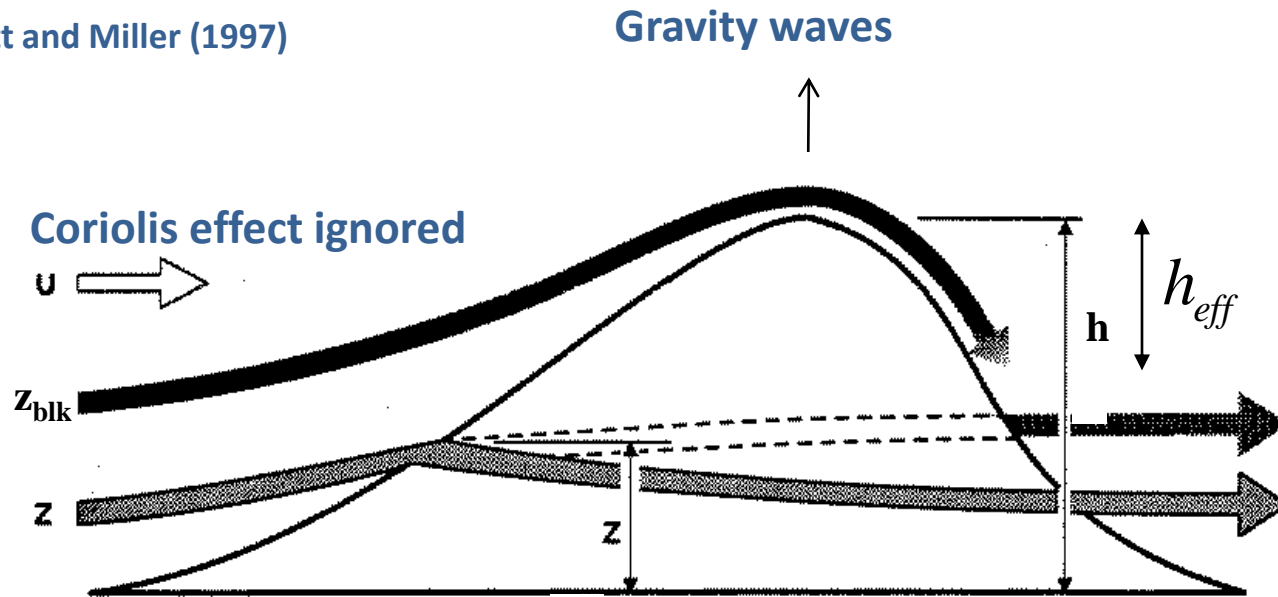


Figure 4: Single lenticular cloud over Laguna Verde, Bolivia. This cloud was probably formed by a vertically propagating mountain wave. (Copyright Bernhard Mühr, www.wolkenatlas.de)

Durran, 2003

What happens if height is not small compared to horizontal scale?

After Lott and Miller (1997)



- linear/flow-over regime (Nh/U small)
- non-linear/blocked regime (Nh/U large)

Blocking occurs if surface air has less kinetic energy than the potential energy barrier presented by the mountain

$$h_{eff} = H_c U / N$$

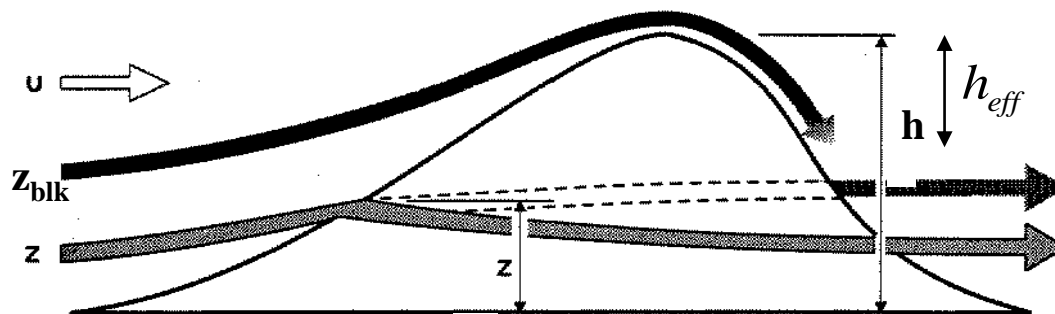
$$z_{blk} = h - h_{eff}$$

Height h_{eff} is such that the Froude number Nh_{eff}/U reaches its critical value H_c

See Hunt and Snyder (1980)

The ECMWF sub-grid orography scheme

- **Horizontal scales smaller than 5 km:** waves are evanescent and flow around steep orographic features will lead to form drag : Turbulent Orographic Form Drag (TOFD, see BL2)
- **Horizontal scales between 5 km and model resolution:** The subgrid orography scheme according to Lott and Miller (1997)
 - Blocking below the blocking height: Strong drag on model levels dependent on geometry of subgrid orography
 - Gravity wave generation by “effective” subgrid mountain height: gravity wave generation dependent on geometry of subgrid orography



The ECMWF sub-grid orography scheme

- Elliptically shaped mountains are assumed with aspect ratio a/b , and orientation ψ with respect to the wind
- Elliptic mountains are equally spaced
- Subgrid orography is characterized by:
 - Standard deviation μ
 - Slope σ
 - Orientation θ
 - Anisotropy γ (1:circular; 0: ridge)

$$\gamma^2 = \frac{K - (L^2 + M^2)^{1/2}}{K + (L^2 + M^2)^{1/2}}$$

$$\theta = 0.5 \tan^{-1}(M / L)$$

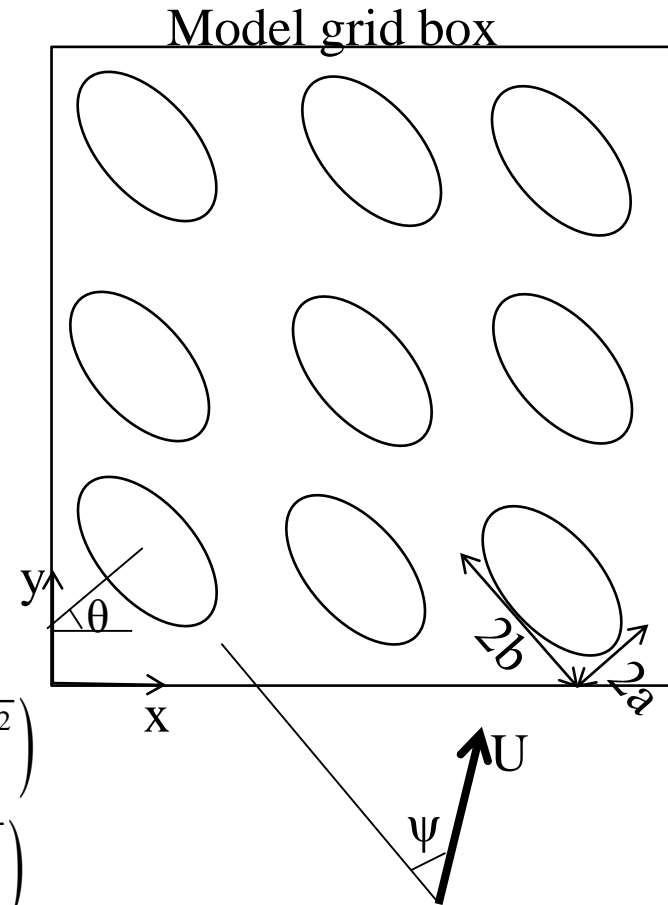
$$\sigma^2 = K + (L^2 + M^2)^{1/2}$$

$$\mu^2 = \overline{h^2} - (\overline{h})^2$$

$$K = 0.5 \left(\overline{(\partial h / \partial x)^2} + \overline{(\partial h / \partial y)^2} \right)$$

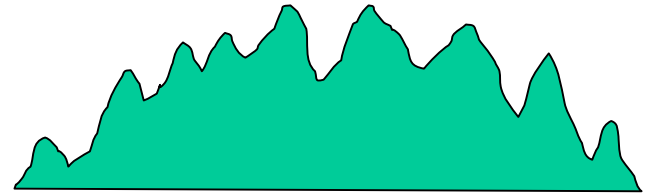
$$L = 0.5 \left(\overline{(\partial h / \partial x)^2} - \overline{(\partial h / \partial y)^2} \right)$$

$$M = \overline{(\partial h / \partial x)(\partial h / \partial y)}$$



Preparation of the data sets to characterize the sub-grid orography

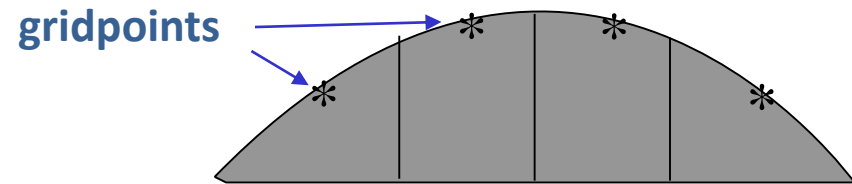
1. Global 1km resolution surface elevation data



2. Reduce to 5 km resolution by smoothing



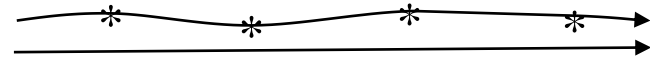
3. Compute mean orography at model resolution



4. Subtract model orography (3) from 5km orography (2)



5. Compute standard deviation, slope, orientation and anisotropy for every grid box



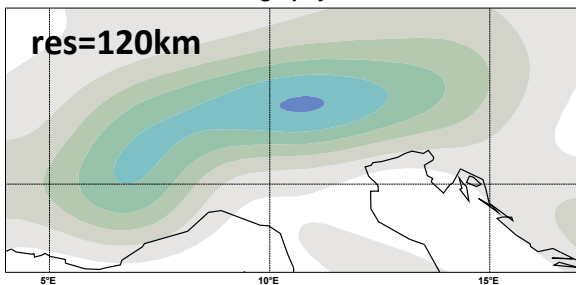
Resolution sensitivity of sub-grid fields

mean orography
/ land sea mask

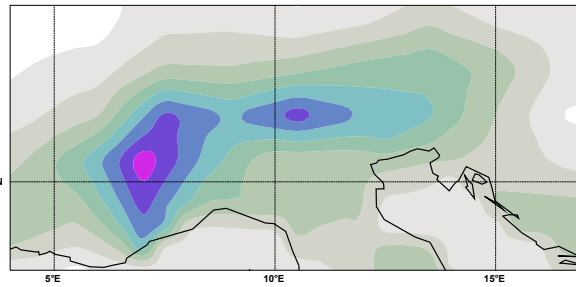
standard deviation (μ)

slope (σ)

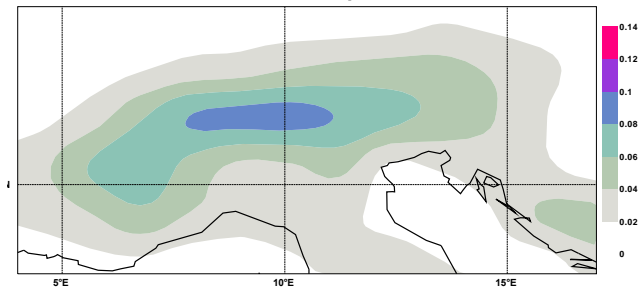
ERA40 mean orography / land sea mask



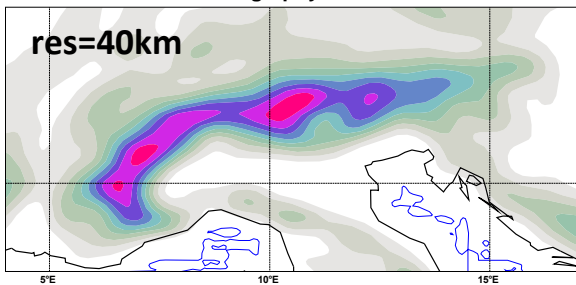
ERA40 standard deviation



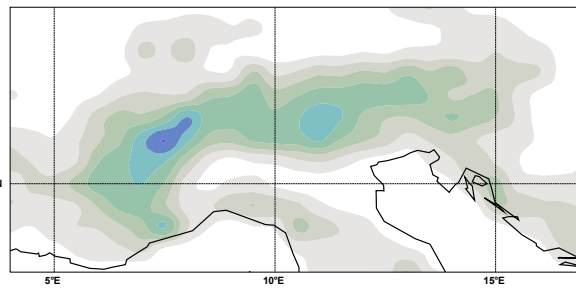
ERA40 slope



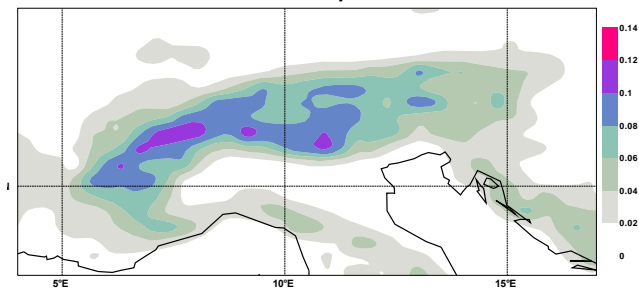
T511 mean orography / land sea mask



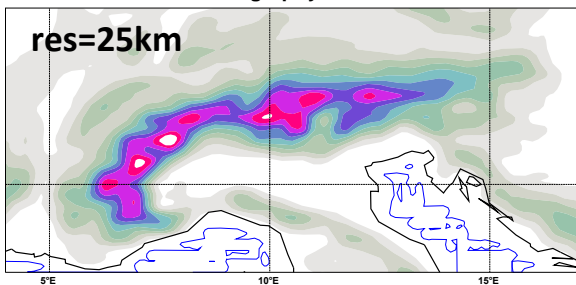
T511 standard deviation



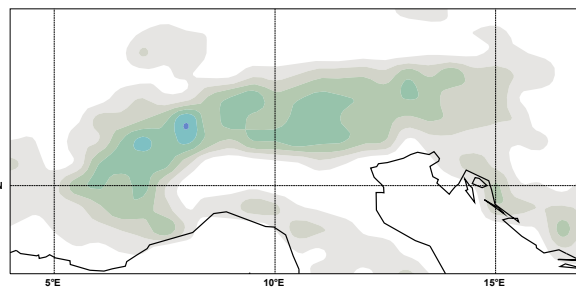
T511 slope



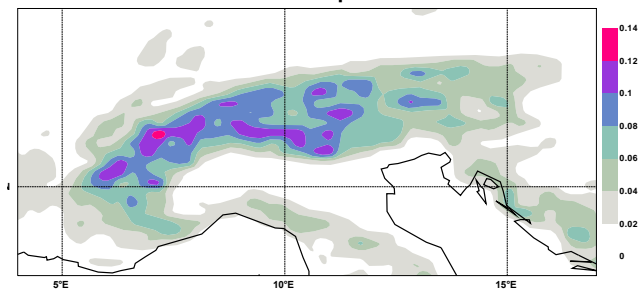
T799 mean orography / land sea mask



T799 standard deviation



T799 slope



Horizontal resolutions: ERA40~120km; T511~40km; T799~25km

The surface drag due to blocking and gravity wave generation

Drag at height z below blocking height applied on model levels:

$$D_{blk}(z) = \rho C_d \max\left(2 - \frac{1}{r}, 0\right) \frac{\sigma}{2\mu} \left(\frac{z_{blk} - z}{z + \mu}\right)^{1/2} (B \cos^2 \psi + C \sin^2 \psi) \frac{U |U|}{2}$$

$$\text{with } r = \frac{\cos^2 \psi + \gamma \sin^2 \psi}{y \cos^2 \psi + \sin^2 \psi}$$

Gravity wave stress above blocking height:

$$\tau_{gwd} = \rho_H U_H N_H h_{eff}^2 \frac{\sigma}{4\mu} G(B \cos^2 \psi_H + C \sin^2 \psi_H, (B - C) \sin \psi_H \cos \psi_H)$$

- B,C,G are constants
 - Index H indicates the characteristic height (2μ)
 - Ψ is computed from θ and wind direction
 - Density of ellipses per grid box is characterized by μ/σ
- μ : Standard deviation
 σ : Slope
 θ : Orientation
 γ : Anisotropy

Gravity wave dissipation

• Strongest dissipation occurs in regions where the wave becomes unstable and breaks down into turbulence, referred to as wave breaking:

- **Convective instability:** where the amplitude of the wave becomes so large that it causes relatively cold air to rise over less dense, warm air

$$N_{\min}^2 = N^2 \left\{ 1 + \frac{N \delta h}{U} \right\}$$

δ : amplitude of wave

N : mean Brunt-Vaisala frequency

- **Kelvin-Helmholtz instability also important:** associated with shear zones. Amplitude of wave is reduced such that Ri_{\min} reaches critical value of 0.25 (saturation hypothesis; Lindzen 1981)

$$Ri_{\min} = \frac{N^2}{\eta^2} = Ri \left\{ \frac{1 - \alpha}{(1 + Ri^{1/2} \alpha^2)^2} \right\}$$

$$\alpha = N |\delta h| / U$$

$$\eta = \partial U / \partial z$$

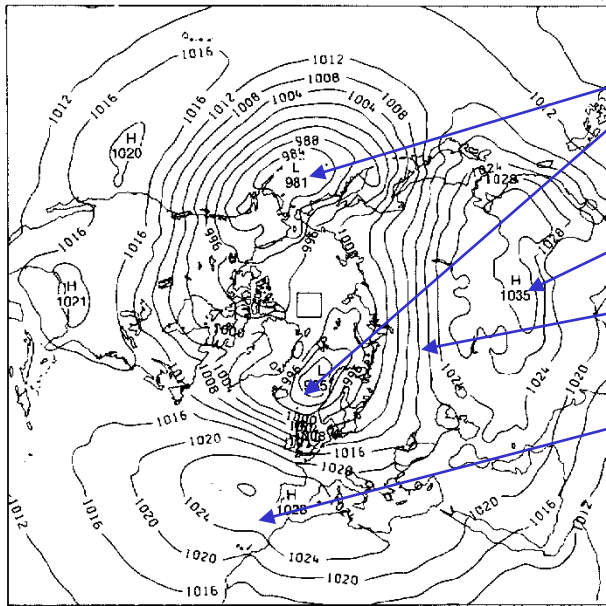
δh : amplitude of wave

Ri : mean Richardson number

Impact of scheme

Alleviation of systematic westerly bias in low resolution model (2.5°x3.75°) in 1985

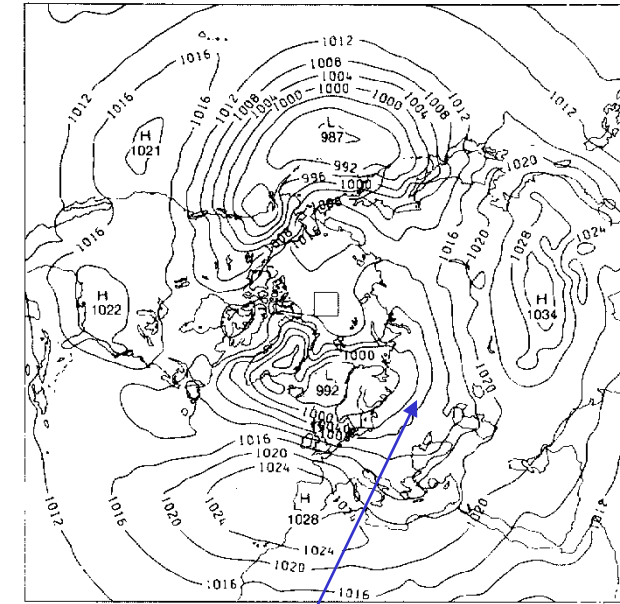
CONTROL EXPERIMENT (C)



Without GWD scheme

Icelandic/Aleutian lows are too deep
Siberian high too weak and too far south
Flow too zonal / westerly bias
Azores anticyclone too far east

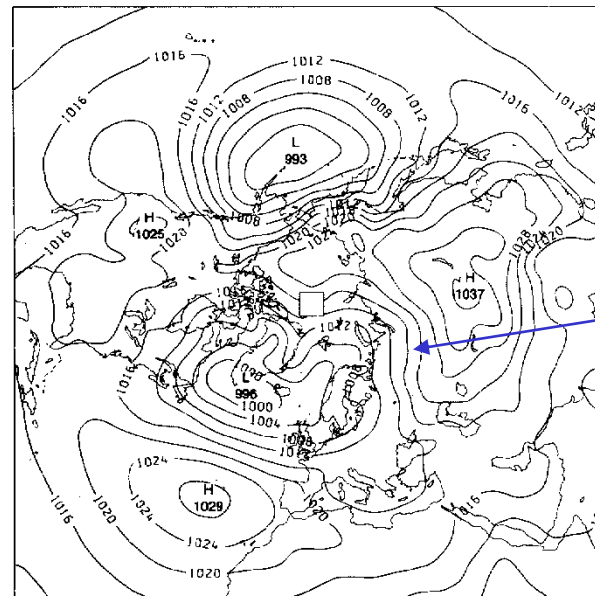
GRAVITY WAVE EXPERIMENT (G)



With GWD scheme

alleviation of westerly bias

MEAN JANUARY 1984-1986



better agreement

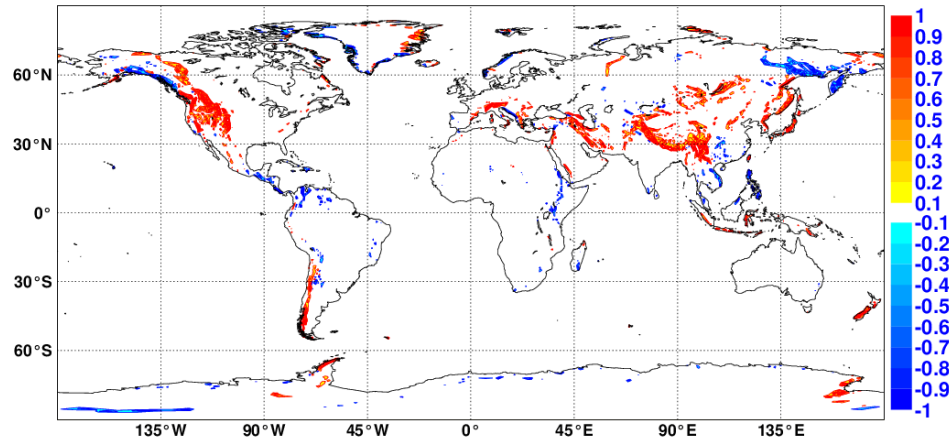
Mean January sea level pressure (mb) for years 1984 to 1986

Analysis (best guess)

Surface stresses averaged over of 26 days (T511L91); Jan 2012

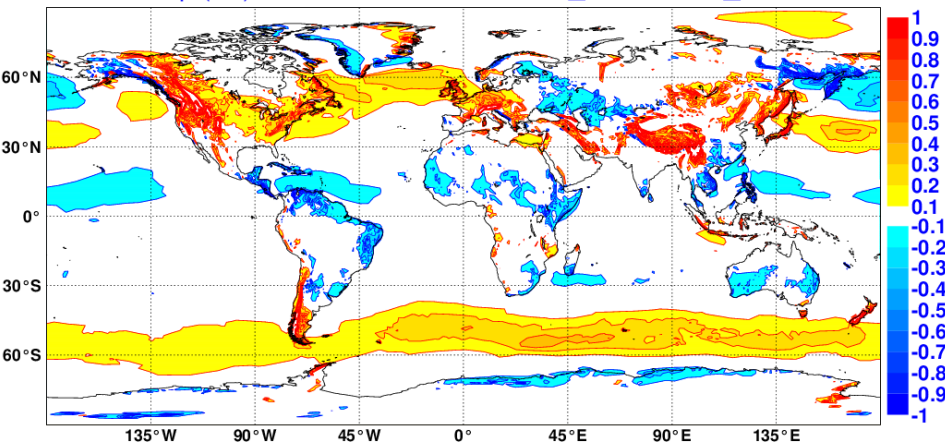
East/West SO stress

LGWS, fvq4(24) 20120106-20120131, GI_av:0, GI_sd:0.07



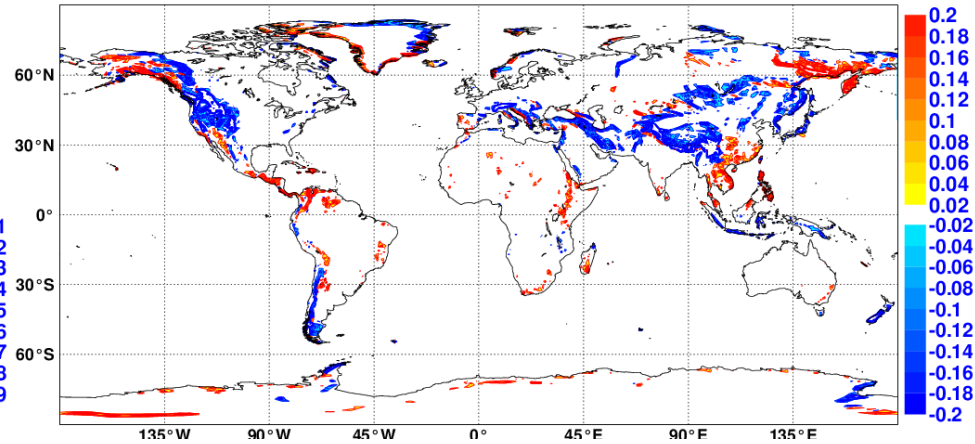
East/West turbulent stress

EWSS, fvq6(24) 20120106-20120131, GI_av:0.02, GI_sd:0.12



East/West turbulent stress difference (SO – no SO)

EWSS_diff, fvq4(24)-fvq6(24); 20120106-20120131, GI_av:0, GI_sd:0.03



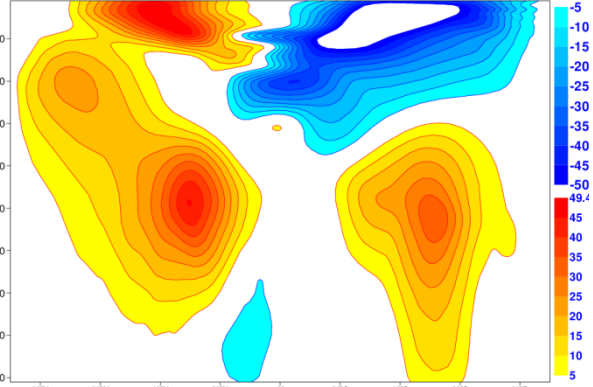
North/South cross section 90N to 90S (averaged over 180W to 180E) averaged of 26 5-day forecasts

U

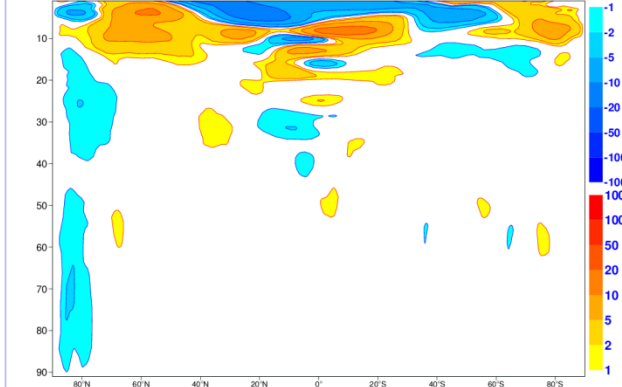
Day-5 U-err without SO

Day-5 U-err with SO

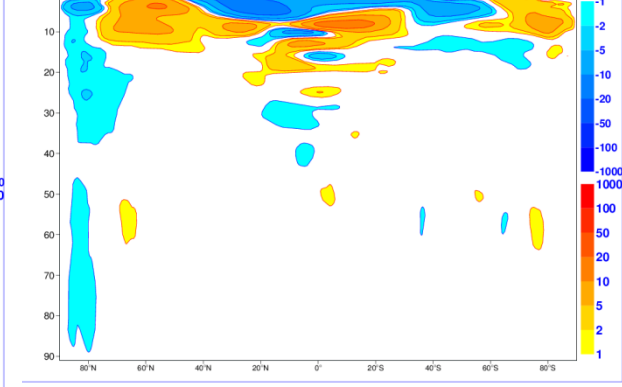
U, fvq6(120) 20120106-20120131; Aver E/W: -180 to 180 deg



U_diff, fvq6(120)-fvq6(0); 20120106-20120131; Aver E/W: -180 to 180 deg



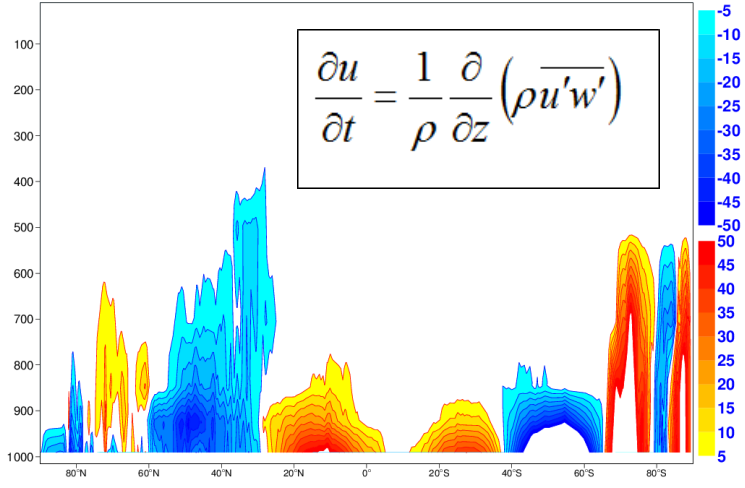
U_diff, fvq4(120)-fvq4(0); 20120106-20120131; Aver E/W: -180 to 180 deg



U-tendency from Turb (m/s/5-days)

U-tend difference: Turb&SO - Turb

96, fvq6(120) 20120106-20120131



0.01 →

1 →

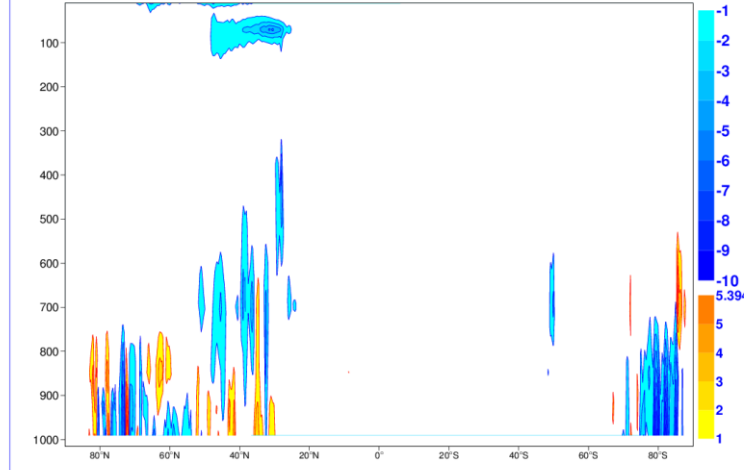
10 →

100 →

500 →

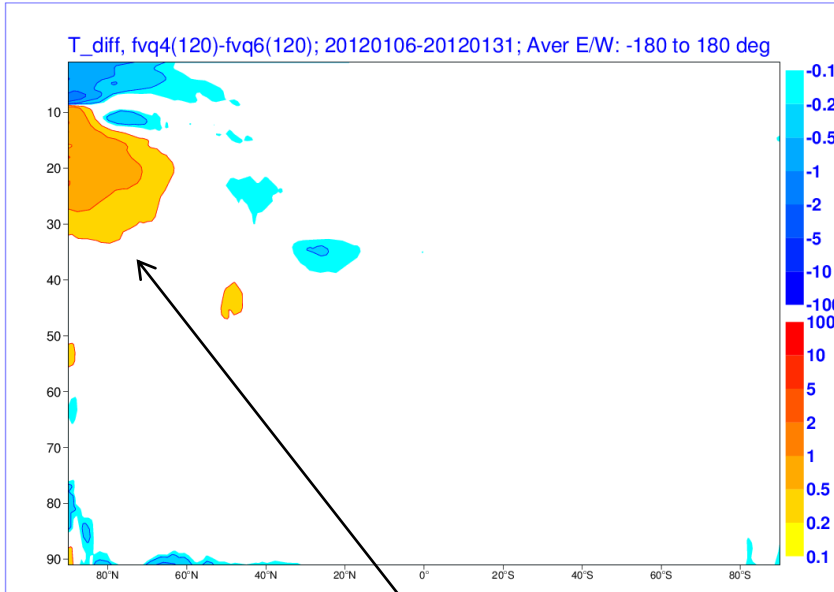
1000 →

96_diff, fvq4(120)-fvq6(120); 20120106-20120131



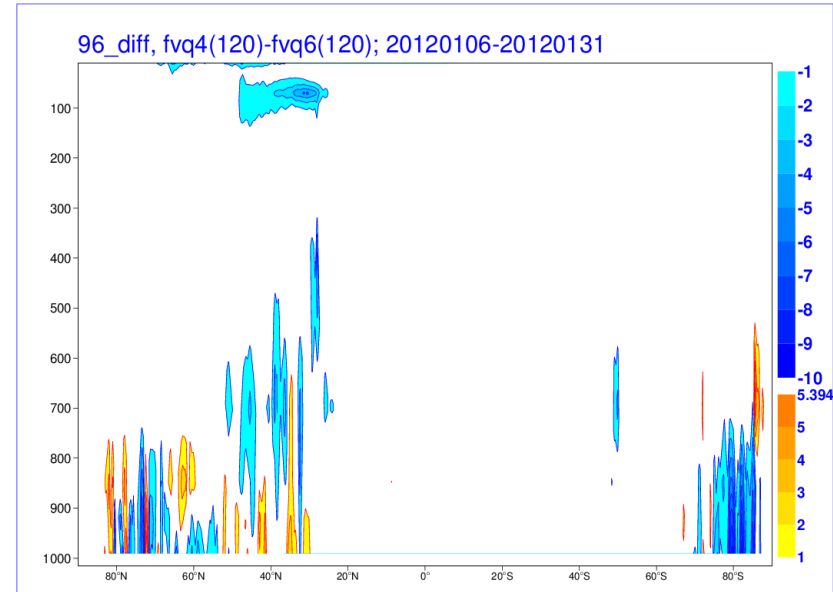
North/South cross section 90N to 90S (averaged over 180W to 180E) averaged of 26 5-day forecasts

Day-5 T-difference: Turb&SO - Turb



U-tend difference: Turb&SO - Turb

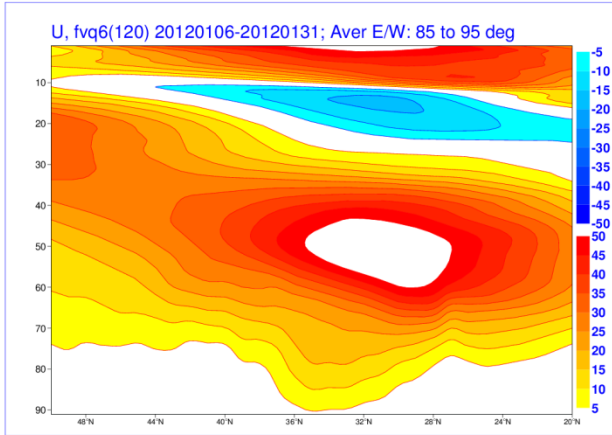
- 0.01 →
- 1 →
- 10 →
- 100 →
- 500 →
- 1000 →



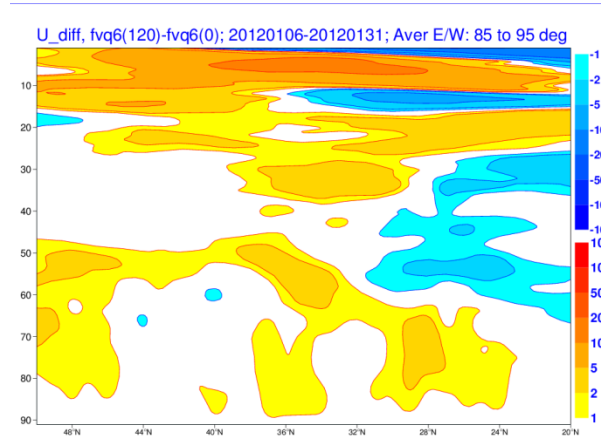
Gravity wave stress in the stratosphere causes a-geostrophic meridional circulation which results in warming in polar stratosphere

North/South cross section 50N to 20N (averaged over 85E to 95E) averaged of 26 5-day forecasts

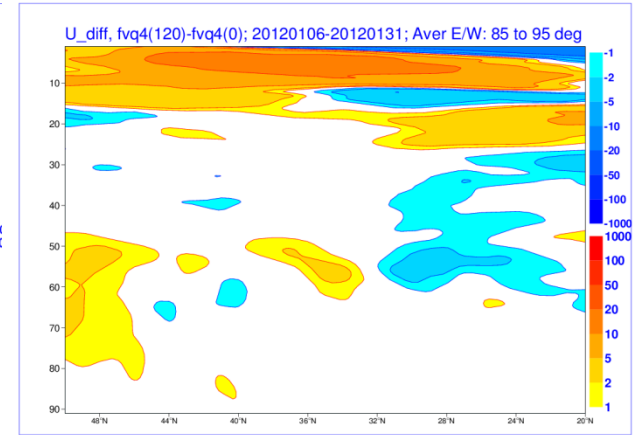
U



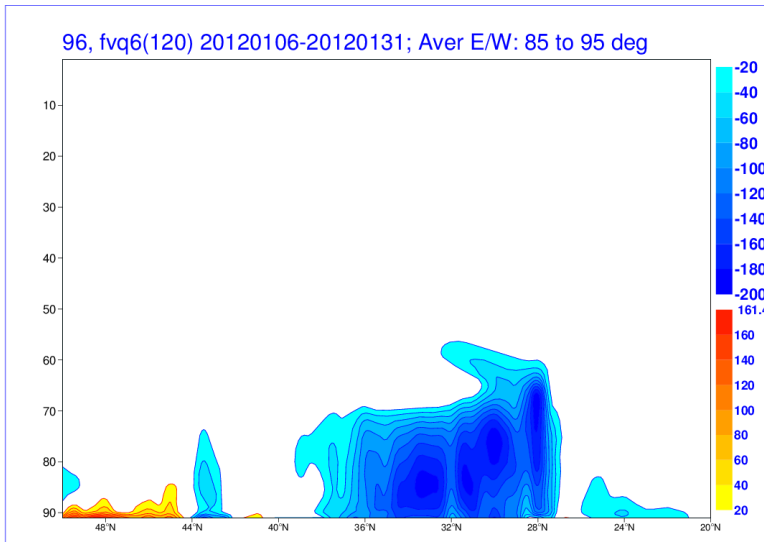
Day-5 U-err without SO



Day-5 U-err with SO

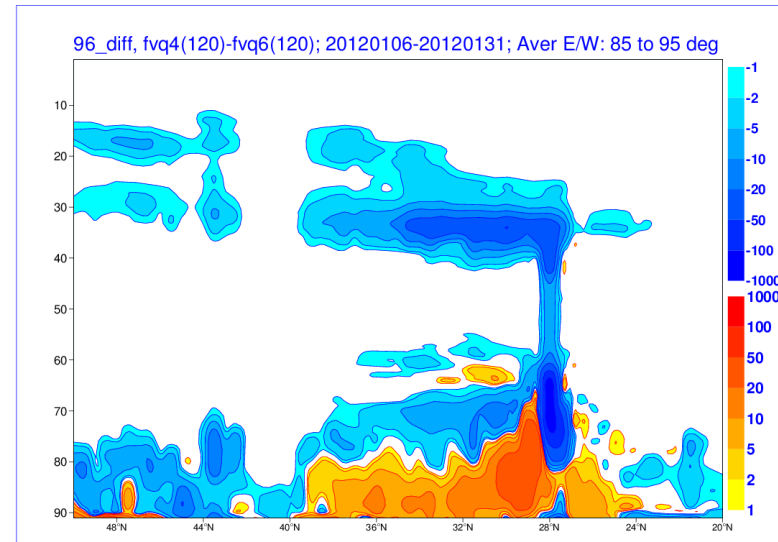


U-tendency from Turb (m/s/5-days)



U-tend difference: Turb&SO - Turb

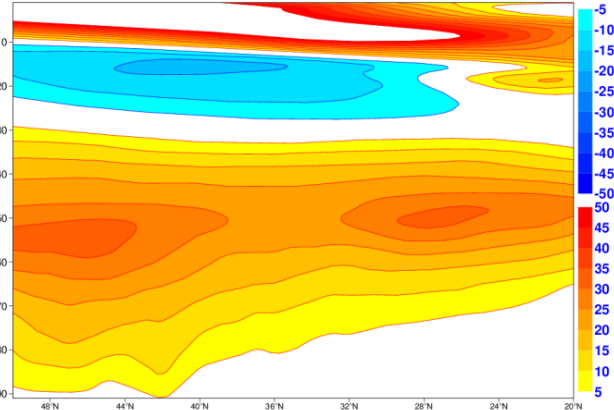
0.01 →
1 →
10 →
100 →
500 →
1000 →



North/South cross section 50N to 20N (averaged over 105W to 115W) averaged of 26 5-day forecasts

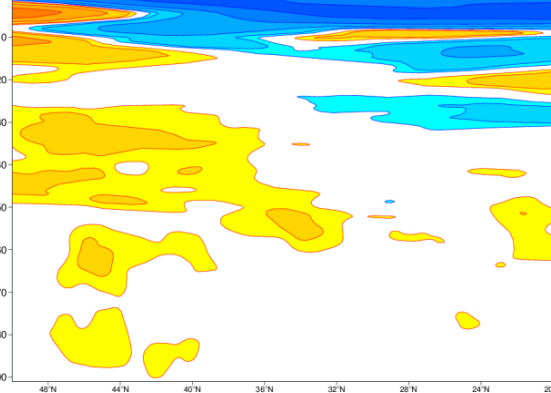
U

U, fvq6(120) 20120106-20120131; Aver E/W: -115 to -105 deg



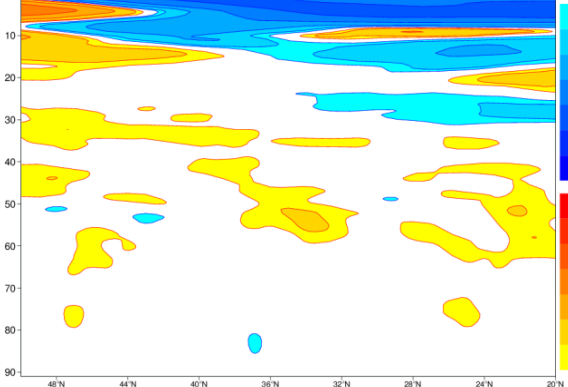
Day-5 U-err without SO

U_diff, fvq6(120)-fvq6(0); 20120106-20120131; Aver E/W: -115 to -105 deg



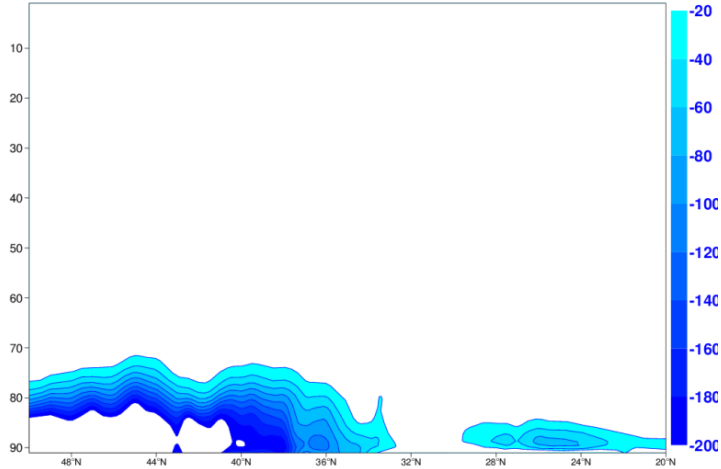
Day-5 U-err with SO

U_diff, fvq4(120)-fvq4(0); 20120106-20120131; Aver E/W: -115 to -105 deg



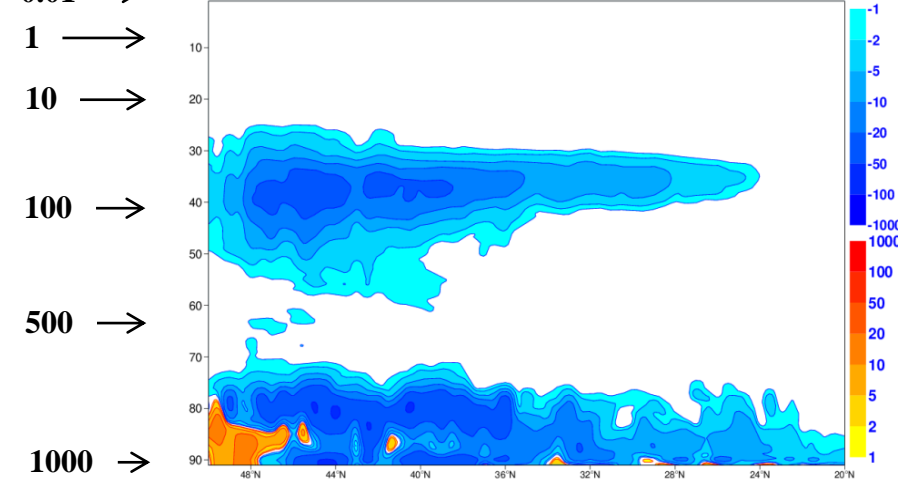
U-tendency from Turb (m/s/5-days)

96, fvq6(120) 20120106-20120131; Aver E/W: -115 to -105 deg



U-tend difference: Turb&SO - Turb

96_diff, fvq4(120)-fvq6(120); 20120106-20120131; Aver E/W: -115 to -105 deg



0.01 →

1 →

10 →

100 →

500 →

1000 →

References

- Alexander, M. J., and H. Teitelbaum, 2007: Observation and analysis of a large amplitude mountain wave event over the Antarctic Peninsula, *J. Geophys. Res.*, 112.
- Bougeault, P., B. Benech, B. Carissimo, J. Pelon, and E. Richard, 1990: Momentum budget over the Pyrenees: The PYREX experiment. *Bull. Amer. Meteor. Soc.*, 71, 806-818.
- Clark, T. L., and M. J. Miller, 1991: Pressure drag and momentum fluxes due to the Alps. II: Representation in large scale models. *Quart. J. R. Met. Soc.*, 117, 527-552.
- Durrán, D. R., 1990: Mountain waves and downslope winds. Atmospheric processes over complex terrain, American Meteorological Society Meteorological Monographs, 23, 59-81.
- Durrán, D. R., 2003: Lee waves and mountain waves, Encyclopedia of Atmospheric Sciences, Holton, Pyle, and Curry Eds., Elsevier Science Ltd.
- Emesis, S., 1990: Surface pressure distribution and pressure drag on mountains. *International Conference of Mountain Meteorology and ALPEX, Garmish-Partenkirchen*, 5-9 June, 1989, 20-22.
- Gregory, D., G. J. Shutts, and J. R. Mitchell, 1998: A new gravity-wave-drag scheme incorporating anisotropic orography and low-level breaking: Impact upon the climate of the UK Meteorological Office Unified Model, *Quart. J. R. Met. Soc.*, 124, 463-493.
- Houze, R. A., 1993: *Cloud Dynamics, International Geophysics Series, Academic Press, Inc.*, 53.
- Hunt, J. C. R., and W. H. Snyder, 1980: Experiments on stably and neutrally stratified flow over a model three-dimensional hill, *J. Fluid Mech.*, 96, 671-704.
- Lilly, D. K., and P. J. Kennedy, 1973: Observations of stationary mountain wave and its associated momentum flux and energy dissipation. *Ibid*, 30, 1135-1152.
- Lott, F. and M. J. Miller, 1997: A new subgrid-scale drag parameterization: Its formulation and testing, *Quart. J. R. Met. Soc.*, 123, 101-127.
- Nappo, C.J., 2002: *An introduction to atmospheric gravity waves*, Academic Press, 276p.
- Olafsson, H., and P. Bougeault, 1996: Nonlinear flows past an elliptic mountain ridge, *J. Atmos. Sci.*, 53, 2465-2489
- Olafsson, H., and P. Bougeault, 1997: The effect of rotation and surface friction on orographic drag, *J. Atmos. Sci.*, 54, 193-210.
- Palmer, T. N., G. J. Shutts, and R. Swinbank, 1986: Alleviation of a systematic westerly bias in general circulation and numerical weather prediction models through an orographic gravity wave drag parameterization, *Quart. J. R. Met. Soc.*, 112, 1001-1039.
- Rontu, L., K. Sattler, R. Sigg, 2002: Parameterization of subgrid-scale orography effects in HIRLAM, HIRLAM technical report, no. 56, 59 pp.
- Rontu, L., 2007, Studies on orographic effects in a numerical weather prediction model, Finish Meteorological Institute, No. 63.
- Scinocca, J. F., and N. A. McFarlane, 2000, :The parameterization of drag induced by stratified flow over anisotropic orography, *Quart. J. R. Met. Soc.*, 126, 2353-2393
- Smith, R. B., 1989: Hydrostatic airflow over mountains. *Advances in Geophysics*, 31, Academic Press, 59-81.
- Smith, R. B., 1979: The influence of mountains on the atmosphere. *Adv. in Geophys.*, 21, 87-230.
- Smith, R. B., S. Skubis, J. D. Doyle, A. S. Broad, C. Christoph, and H. Volkert, 2002: Mountain waves over Mont Blanc: Influence of a stagnant boundary layer. *J. Atmos. Sci.*, 59, 2073-2092.
- Smith, S., J. Doyle., A. Brown, and S. Webster, 2006: Sensitivity of resolved mountain drag to model resolution for MAP case studies. *Quart. J. R. Met. Soc.*, 132, 1467-1487.
- Vosper, S., and S. Mobbs: Numerical simulations of lee-wave rotors.